



# Csp1, a Cold Shock Protein Homolog in *Xylella fastidiosa* Influences Cell Attachment, Pili Formation, and Gene Expression

 Wei Wei,<sup>a</sup> Teresa Sawyer,<sup>b</sup> Lindsey Burbank<sup>a</sup>

<sup>a</sup>USDA Agricultural Research Service, San Joaquin Valley Agricultural Sciences Center, Parlier, California, USA

<sup>b</sup>Electron Microscopy Facility, Oregon State University, Corvallis, Oregon, USA

**ABSTRACT** Bacterial cold shock-domain proteins are conserved nucleic acid binding chaperones that play important roles in stress adaptation and pathogenesis. Csp1 is a temperature-independent cold shock protein homolog in *Xylella fastidiosa*, a bacterial plant pathogen of grapevine and other economically important crops. Csp1 contributes to stress tolerance and virulence in *X. fastidiosa*. However, besides general single-stranded nucleic acid binding activity, little is known about the specific function(s) of Csp1. To further investigate the role(s) of Csp1, we compared phenotypic differences and transcriptome profiles between the wild type and a *csp1* deletion mutant ( $\Delta csp1$ ). Csp1 contributes to attachment and long-term survival and influences gene expression. We observed reduced cell-to-cell attachment and reduced attachment to surfaces with the  $\Delta csp1$  strain compared to those with the wild type. Transmission electron microscopy imaging revealed that  $\Delta csp1$  was deficient in pili formation compared to the wild type and complemented strains. The  $\Delta csp1$  strain also showed reduced survival after long-term growth *in vitro*. Long-read nanopore transcriptome sequencing (RNA-Seq) analysis revealed changes in expression of several genes important for attachment and biofilm formation in  $\Delta csp1$  compared to that in the wild type. One gene of interest, *pilA1*, which encodes a type IV pili subunit protein, was upregulated in  $\Delta csp1$ . Deleting *pilA1* in *X. fastidiosa* strain Stag's Leap increased surface attachment *in vitro* and reduced virulence in grapevines. *X. fastidiosa* virulence depends on bacterial attachment to host tissue and movement within and between xylem vessels. Our results show that the impact of Csp1 on virulence may be due to changes in expression of attachment genes.

**IMPORTANCE** *Xylella fastidiosa* is a major threat to the worldwide agriculture industry. Despite its global importance, many aspects of *X. fastidiosa* biology and pathogenicity are poorly understood. There are currently few effective solutions to suppress *X. fastidiosa* disease development or eliminate bacteria from infected plants. Recently, disease epidemics due to *X. fastidiosa* have greatly expanded, increasing the need for better disease prevention and control strategies. Our studies show a novel connection between cold shock protein Csp1 and pili abundance and attachment, which have not been reported for *X. fastidiosa*. Understanding how pathogenesis-related gene expression is regulated can aid in developing novel pathogen and disease control strategies. We also streamlined a bioinformatics protocol to process and analyze long-read nanopore bacterial RNA-Seq data, which will benefit the research community, particularly those working with non-model bacterial species.

**KEYWORDS** RNA-seq, *Xylella fastidiosa*, biofilms, cold shock proteins, gene expression, plant pathogens, stress response, transcriptional regulation, type IV pili, virulence factors

**X***ylella fastidiosa* is an economically important plant pathogen that causes disease in many agricultural crops, including grapevines, citrus, almonds, alfalfa, and coffee. Infection of grapevines by *X. fastidiosa* subsp. *fastidiosa* is known as Pierce's disease (1–6). Pierce's disease is a serious problem for the grapevine industry in the United States,

**Citation** Wei W, Sawyer T, Burbank L. 2021. Csp1, a cold shock protein homolog in *Xylella fastidiosa* influences cell attachment, pili formation, and gene expression. Microbiol Spectr 9:e01591-21. <https://doi.org/10.1128/Spectrum.01591-21>.

**Editor** Jeffrey A. Gralnick, University of Minnesota

This is a work of the U.S. Government and is not subject to copyright protection in the United States. Foreign copyrights may apply.

Address correspondence to Wei Wei, wei.wei2@usda.gov.

**Received** 21 September 2021

**Accepted** 7 October 2021

**Published** 17 November 2021

especially in California, where the disease threatens the \$30 billion wine industry (7). During the infection cycle, *X. fastidiosa* is spread via sap-feeding insect vectors and colonizes the xylem tissue of plants (8). In the plant xylem, the bacteria encounter many stressors, such as plant defense responses, that can reduce pathogen viability. Abiotic stressors, such as cold temperature, can also affect long-term survival of the bacteria in grapevines and have been linked to pathogen elimination and vine recovery (9, 10).

The Csp superfamily consists of a diverse group of homologous proteins conserved in many bacteria (11). Most research on bacterial cold shock proteins have focused on their role in helping bacteria adapt and survive at suboptimal temperatures; however, several studies show that some Csps also contribute to virulence and general stress response (12–15). *X. fastidiosa* subsp. *fastidiosa* Csp1 shares 53% amino acid sequence identity with CspA from *Escherichia coli* K-12 (ECDH10B\_3735) and 52% identity with a CspA homolog (XC\_1828) from *Xanthomonas campestris* pv. *campestris* (16). In *E. coli*, some Csps have been identified as paralogs (CspA and CspB, CspH and CspF, CspC and CspE, CspI and CspG) (2). Five of the nine *E. coli* Csps (CspA, CspB, CspE, CspG, and CspI) are induced by changes in temperature (11), while CspC and CspE are constitutively expressed at normal growth temperatures (37°C) and are involved in regulating stress response gene expression (17). *E. coli* CspD is induced at early stationary phase and is important for survival under nutrient-poor conditions (15). Previous studies on *X. fastidiosa* Stag's Leap revealed that deleting *csp1* resulted in reduced survival after cold treatment *in vitro*; however, *csp1* expression is not induced by cold exposure, and its importance to *X. fastidiosa* cold survival *in planta* is not as well established (16). Csp1 is also important for osmotic stress tolerance (16). These results suggest that, like *E. coli* CspE and CspC, *X. fastidiosa* Csp1 may be less important for cold survival and play a more prominent role in general stress tolerance.

In some animal and plant pathogens, Csps are also important for regulation of virulence factors. A triple deletion mutant ( $\Delta cspABD$ ) in bacterial foodborne pathogen *Listeria monocytogenes* reduced oxidative and cold stress survival and impaired host cell invasion and intracellular growth (13). The *L. monocytogenes*  $\Delta cspABD$  mutant was also deficient in cellular aggregation and did not express surface flagella or exhibit swarming motility (18). Gene expression analysis showed reduced expression of virulence and motility genes in *L. monocytogenes* *csp* mutants, suggesting that some Csps may regulate gene expression. Similarly, some cold shock proteins in plant-pathogenic bacteria also act as virulence factors and regulate gene expression. The *Xanthomonas oryzae* pv. *oryzae* (*Xoo*) CspA protein regulates expression of two virulence genes, *PXO\_RS11830* and *PXO\_RS01060* (14). Deletion of *Xoo cspA* decreased cold tolerance, bacterial pathogenicity, biofilm formation, and polysaccharide production (14). In *X. fastidiosa* strain Stag's Leap, deleting *csp1* resulted in significantly reduced disease severity and bacterial titer in the absence of cold stress in susceptible Chardonnay grapevines (16). However, the mechanisms of how Csp1 contributes to virulence are not well understood.

In this study, we investigated the molecular mechanisms through which *X. fastidiosa* Csp1 contributes to stress tolerance and virulence. Since the *X. fastidiosa* *csp1* mutant was less tolerant to certain stress conditions and had a bacterial titer lower than that of the wild type *in planta* (16), we compared long-term survival of wild-type *X. fastidiosa* Stag's Leap with that of the  $\Delta csp1$  mutant and a complemented strain. We also investigated whether Csp1 influences biofilm formation since xylem occlusion by biofilms is a major aspect of *X. fastidiosa* pathogenicity, and the  $\Delta csp1$  mutant produced less-severe symptoms in grapevine compared to the wild type (16). Last, because Csp1 has general nucleic acid binding activity (16) and studies in other bacteria show that some Csps regulate gene expression, we also investigated the influence of Csp1 on *X. fastidiosa* gene expression using transcriptome sequencing (RNA-Seq) to compare transcriptomes of wild-type Stag's Leap and the  $\Delta csp1$  mutant.

## RESULTS

***X. fastidiosa*  $\Delta csp1$  mutant showed reduced long-term survival *in vitro*.** Previous work showed that deleting the *csp1* gene in *X. fastidiosa* strain Stag's Leap resulted in

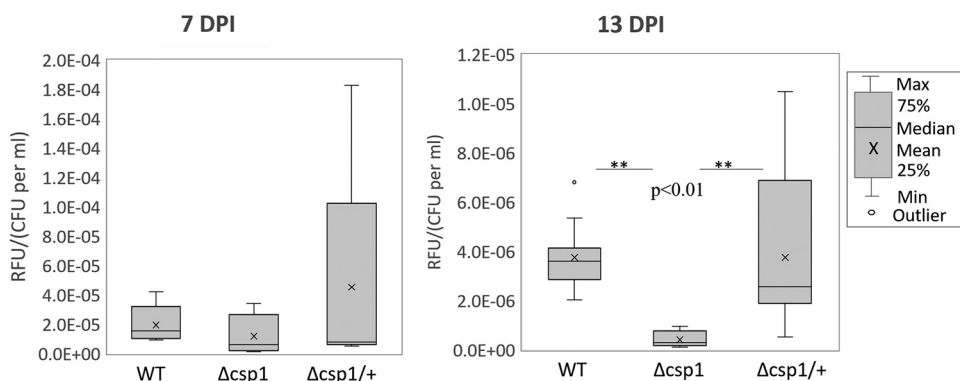


**FIG 1** Cell viability of the  $\Delta csp1$  during long-term growth. Wild-type Stag's Leap,  $\Delta csp1$ , and  $\Delta csp1/csp1+$  were grown on PD3 plates for up to 13 days. Cell viability was quantified at 7 days postinoculation (DPI) and 13 DPI using alamarBlue (Life Technologies) fluorescent cell viability reagent by measuring relative fluorescent units (RFU) of each sample and normalizing to total cells quantified by qPCR. Graph represents data collected from at least three independent experiments. \*\*, treatment significantly different from the wild type based on one-way analysis of variance (ANOVA) followed by Tukey means comparison test ( $P < 0.01$ ).

reduced tolerance to salt and cold stress (16). Since these results strongly suggest that Csp1 may play a role in *X. fastidiosa* stress adaptation, we were interested to see if Csp1 was involved in survival under other stresses, such as prolonged survival times. We compared cell viability of wild-type,  $\Delta csp1$ , and  $\Delta csp1/csp1+$  strains grown on PD3 plates at 7 days postinoculation (DPI), when *X. fastidiosa* cells begin to decline, and at 13 DPI (extended stationary phase). No significant change in viability was observed between the mutant and the wild type at 7 days postinoculation (DPI) (Fig. 1), but there was a significant decrease in viability of  $\Delta csp1$  at 13 DPI compared to that of the wild-type and complemented strains (Fig. 1). The *csp1* mutant grows at a rate comparable to that of the wild-type and complemented strains at earlier time points (Fig. S1). These results suggest that Csp1 is important for long-term or stationary-phase survival of *X. fastidiosa* *in vitro*.

**$\Delta csp1$  strain showed reduced cellular aggregation and surface adhesion.** Biofilm formation is an important aspect of *X. fastidiosa* host colonization and involves both cell-cell aggregation and cellular adhesion to surfaces (19). Wild-type Stag's Leap cells form visible aggregates and a biofilm ring at the air-liquid interface when grown in liquid PD3 medium (Fig. 2A). However, the  $\Delta csp1$  mutant showed a dispersed phenotype with visibly fewer cells attached at the air-liquid interface when grown under the same conditions as the wild type (WT) and the complemented strains (Fig. 2A). We quantified and compared aggregation of the WT,  $\Delta csp1$ , and  $\Delta csp1/csp1+$  strains and found that the percentage of aggregated cells in liquid culture was significantly lower for  $\Delta csp1$  than for the WT and complemented strains (Fig. 2B). In addition to cellular aggregation, biofilm formation also requires cell adhesion to surfaces. We quantified surface attachment of static cultures of WT,  $\Delta csp1$ , and  $\Delta csp1/csp1+$  strains grown in 96-well plates using crystal violet staining and observed a significant decrease in the number of attached cells for the mutant strain compared to that for the WT and the complemented strains (Fig. 2C).

**$\Delta csp1$  mutant shows reduced pili formation.** *X. fastidiosa* pili are important for cellular aggregation and surface attachment (20). To evaluate the effect of *csp1* on pilus formation, cells of the wild type Stag's Leap, the  $\Delta csp1$  mutant, and the complemented strains were visualized using transmission electron microscopy (TEM), as shown in Figure 3. TEM images of wild-type *X. fastidiosa* show that pili localized to one pole of the cell, while the *csp1* mutant did not show visible pili formation (Fig. 3). The complemented strain shows restored pilus formation, with most of the pili concentrated toward one pole of the cell (Fig. 3).

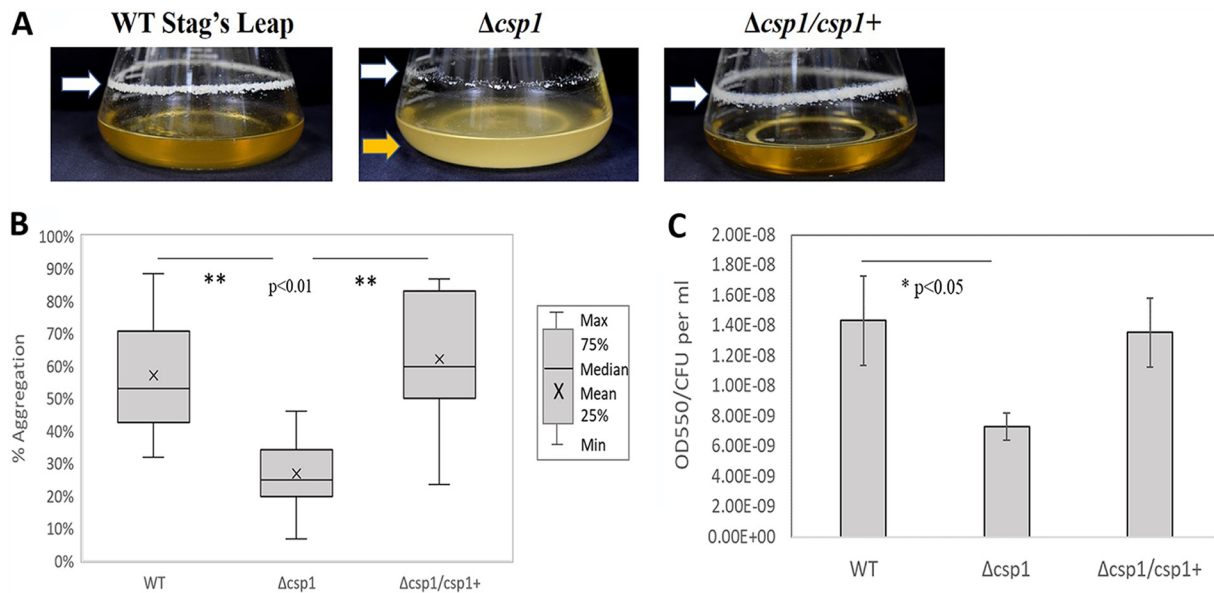


**FIG 2** Cellular aggregation and attachment of  $\Delta csp1$  *in vitro*. (A) Cell-cell aggregation and surface attachment was documented after 4 days of growth in liquid PD3 medium at 28°C with shaking at 180 rpm. The yellow arrow indicates the dispersed phenotype of the  $\Delta csp1$  strain, and the white arrows indicate the ring of attached cells at the air-liquid interface. (B) Cellular aggregation was quantified by measuring the  $OD_{600}$  of statically grown liquid cultures of WT,  $\Delta csp1$ , and  $\Delta csp1/csp1+$  before and after manual dispersal of cells using the equation  $[(OD_{600D} - OD_{600U})/OD_{600D}] \times 100$ , where  $OD_{600D}$  is optical density of dispersed culture and  $OD_{600U}$  is optical density of undispersed culture. The graph represents a total of at least nine replicates from three separate experiments. \*\*, significant difference based on one-way ANOVA followed by Tukey means comparison test ( $P < 0.01$ ). (C) Cell attachment was quantified by measuring the amount of crystal violet stain retained by cells attached to the walls of 96-well plates ( $OD_{550}$ ) after static growth for 4 days.  $OD_{550}$  was normalized to total cells (CFU/ml quantified by qPCR). Graph represents at least 45 technical replicates from three separate experiments. \*, significant difference ( $P < 0.05$ ) from wild type based on one-way ANOVA followed by Bonferroni-Holm.

**Motility- and attachment-related genes were differentially expressed in the  $\Delta csp1$  strain.** To investigate the influence of Csp1 on *X. fastidiosa* gene expression, we used nanopore RNA-Seq to sequence transcriptomes of wild-type *X. fastidiosa* strain Stag's Leap and the  $\Delta csp1$  deletion mutant under standard growth conditions (28°C). RNA-Seq analysis revealed that 90 genes were expressed differentially in the  $\Delta csp1$  strain compared to the wild type (Table 1). Of the 90 differentially expressed genes, 65 were downregulated and 25 were upregulated in  $\Delta csp1$  compared to the wild type. The RNA-Seq results also showed that no transcripts mapped to the *csp1* gene in the mutant strain, verifying that *csp1* was absent and showing the accuracy of transcript mapping (Table 1). Gene ontology analysis using GSEA Pro (<http://gseapro.molgenrug.nl/>) showed significant enrichment of genes involved in cell adhesion/attachment, gene regulation, translation, and rRNA binding. To identify genes of interest for further investigation, we focused on genes that may be associated with phenotypes observed in the  $\Delta csp1$  mutant, such as reduced cellular aggregation and attachment and the

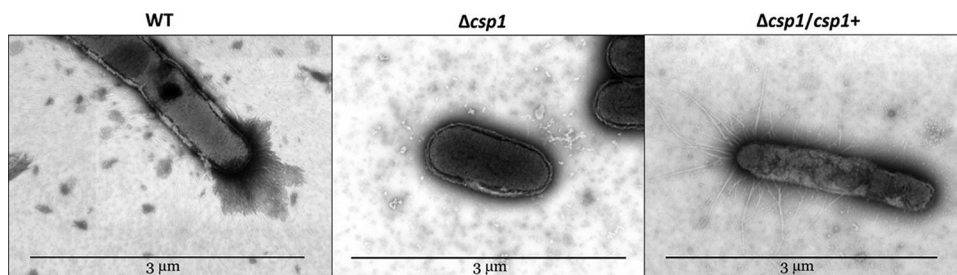


**FIG 3** TEM images of *X. fastidiosa* strains. Pili location and abundance were observed for wild-type Stag's Leap (WT), the *csp1* mutant ( $\Delta csp1$ ), and the complemented ( $\Delta csp1/csp1+$ ) strains using the Helios NanoLab 650 microscope.

**TABLE 1** Differentially expressed genes

Locus ID	Gene symbol	Product	Transcripts per million		Expression ratio ( $\Delta csp1$ /WT)
			WT	$\Delta csp1$	
PD0020	<i>pilV</i>	Pre-pilin leader sequence	180.08	0.00	0.00
PD0141	<i>fabG</i>	3-Ketoacyl-(acyl-carrier-protein) reductase	127.23	0.00	0.00
PD1354		Hypothetical protein	2,582.82	0.00	0.00
PD1380	<i>csp1</i>	Cold shock protein	5,290.81	0.00	0.00
PD1701	<i>dnaB</i>	Replicative DNA helicase	44.29	0.00	0.00
PD1735	<i>fimT</i>	Type 4 fimbrial biogenesis protein	131.92	0.00	0.00
PD1944	<i>rpsR</i>	30S ribosomal protein S18	8,011.60	0.00	0.00
PD2095		Hypothetical protein	119.23	0.00	0.00
PD1926	<i>pilA2</i>	Fimbrial protein	2,184.57	66.44	0.03
PD0216	<i>cvaC</i>	Colicin V precursor	10,631.85	842.10	0.08
PD1931	<i>sucD</i>	Succinyl-CoA synthetase subunit alpha	133.48	11.68	0.09
PD1317		Hypothetical protein	112.39	10.34	0.09
PD1905	<i>xrvA</i>	Virulence regulator	492.63	46.72	0.09
PD2003	<i>rplJ</i>	50S ribosomal protein L10	479.16	45.72	0.10
PD0463		Hypothetical protein	2,108.37	201.98	0.10
PD0084	<i>rplS</i>	50S ribosomal protein L19	947.68	115.89	0.12
PD1945	<i>rpsF</i>	30S ribosomal protein S6	1,201.60	179.24	0.15
PD1063		Hypothetical protein	1,287.41	202.47	0.16
PD0556		Hypothetical protein	28,667.31	4,555.29	0.16
PD0062	<i>fimA</i>	Fimbrial subunit precursor	10,009.57	1,724.44	0.17
PD0217		Hypothetical protein	2,815.96	511.29	0.18
PD1440	<i>rpsT</i>	30S ribosomal protein S20	6,060.28	1,246.99	0.21
PD0708		Virulence regulator	672.31	141.02	0.21
PD1914	<i>rpmI</i>	50S ribosomal protein L35	21,603.77	4,619.53	0.21
PD0626	<i>ssb</i>	Single-stranded DNA-binding protein	484.98	103.71	0.21
PD0061	<i>fimC</i>	Chaperone protein precursor	477.40	108.95	0.23
PD1087		Hypothetical protein	2,361.29	585.51	0.25
PD0283	<i>dksA</i>	DnaK suppressor	927.35	238.22	0.26
PD0313	<i>pspB</i>	Serine protease	76.39	19.88	0.26
PD0459	<i>rpsK</i>	30S ribosomal protein S11	2,578.30	684.46	0.27
PD0460	<i>rpsD</i>	30S ribosomal protein S4	949.37	255.44	0.27
PD1913	<i>rplT</i>	50S ribosomal protein L20	2,372.81	665.13	0.28
PD0447	<i>rplN</i>	50S ribosomal protein L14	2,169.26	615.27	0.28
PD2122	<i>rnpA</i>	Ribonuclease P	1,479.05	424.04	0.29
PD2121	<i>yidC</i>	Putative inner membrane protein translocase component YidC	96.10	30.18	0.31
PD0453	<i>rplR</i>	50S ribosomal protein L18	1,681.26	541.74	0.32
PD1684		Hypothetical protein	15,592.41	5,202.73	0.33
PD0462	<i>rplQ</i>	50S ribosomal protein L17	1,407.81	481.26	0.34
PD0458	<i>rpsM</i>	30S ribosomal protein S13	2,889.36	991.26	0.34
PD1557	<i>apbE</i>	Thiamine biosynthesis lipoprotein ApbE precursor	132.21	46.45	0.35
PD1807	<i>ompW</i>	Outer membrane protein	3,923.03	1,396.21	0.36
PD0442	<i>rplV</i>	50S ribosomal protein L22	2,512.05	900.32	0.36
PD0856	<i>dcp</i>	Peptidyl-dipeptidase	111.54	42.17	0.38
PD1808		Hypothetical protein	35,966.82	13,605.11	0.38
PD0824	<i>hsf/xadA</i>	Afimbrial adhesin surface protein	43.10	16.51	0.38
PD0464	<i>comM</i>	Competence-related protein	257.79	98.85	0.38
PD1993	<i>csp2</i>	Temp acclimation protein B	97,359.93	38,394.08	0.39
PD0246	<i>secG</i>	Preprotein translocase subunit SecG	1,557.96	650.10	0.42
PD0436	<i>rpsJ</i>	30S ribosomal protein S10	7,969.22	3,538.88	0.44
PD1984	<i>gacA</i>	Transcriptional regulator	694.76	310.36	0.45
PD0448	<i>rplX</i>	50S ribosomal protein L24	2,529.90	1,134.00	0.45
PD1558	<i>comE</i>	DNA transport competence protein	16,765.37	7,555.53	0.45
PD1709	<i>mopB</i>	Outer membrane protein	597.52	309.74	0.52
PD2123	<i>rpmH</i>	50S ribosomal protein L34	36,412.20	19,544.34	0.54
PD0446	<i>rpsQ</i>	30S ribosomal protein S17	11,515.54	6,378.49	0.55
PD0451	<i>rpsH</i>	30S ribosomal protein S8	3,394.73	1,983.09	0.58
PD0060	<i>fimD</i>	Outer membrane usher protein precursor	75.88	46.68	0.62
PD0452	<i>rplF</i>	50S ribosomal protein L6	1,627.21	1,022.85	0.63
PD0461	<i>rpoA</i>	DNA-directed RNA polymerase subunit alpha	477.69	301.63	0.63
PD0159		Hypothetical protein	1,722.76	1,188.73	0.69

(Continued on next page)

**TABLE 1** (Continued)

Locus ID	Gene symbol	Product	Transcripts per million		Expression ratio ( $\Delta csp1$ /WT)
			WT	$\Delta csp1$	
PD1506		Hemolysin-type calcium binding protein	44.91	33.05	0.74
PD0443	<i>rpsC</i>	30S ribosomal protein S3	1,071.77	882.49	0.82
PD0437	<i>rplC</i>	50S ribosomal protein L3	902.22	780.56	0.87
PD2001	<i>rpoB</i>	DNA-directed RNA polymerase subunit beta	132.27	117.96	0.89
PD0444	<i>rplP</i>	50S ribosomal protein L16	2,534.48	2,298.26	0.91
PD1467		Hypothetical protein	33.00	104.77	3.18
PD0887	<i>ruvA</i>	Holliday junction DNA helicase RuvA	185.24	613.78	3.31
PD0718	<i>nodQ</i>	Bifunctional sulfate adenylyltransferase subunit 1/adenylylsulfate kinase protein	96.67	322.35	3.33
PD1589	<i>btuB</i>	TonB-dependent receptor	21.48	86.50	4.03
PD0179		Hypothetical protein	21.64	92.00	4.25
PD1652	<i>recB</i>	Exodeoxyribonuclease V beta chain	4.63	19.88	4.29
PD1167	<i>ugd</i>	UDP-glucose dehydrogenase	41.30	177.84	4.31
PD1924	<i>pilA1</i>	Fimbrial protein	202.45	892.96	4.41
PD1702		Hypothetical protein	80.27	362.95	4.52
PD0744	<i>hsf</i>	Surface protein	22.05	114.75	5.20
PD1829	<i>xylA</i>	Family 3 glycoside hydrolase	4.24	22.78	5.37
PD1703		Hypothetical protein	82.67	492.01	5.95
PD0405	<i>rpfG</i>	Response regulator	44.40	271.61	6.12
PD0292	<i>argE</i>	Acetylmethionine deacetylase	13.64	89.63	6.57
PD1517		Hypothetical protein	52.15	349.41	6.70
PD1280	<i>hspA</i>	Low mol wt heat shock protein	832.27	5,951.42	7.15
PD1409	<i>grx</i>	Glutaredoxin-like protein	76.86	559.19	7.28
PD0521		Hypothetical protein	946.01	7,042.88	7.44
PD1850		M20/M25/M40 family peptidase	13.43	107.39	7.99
PD1531		Hypothetical protein	538.53	5,090.18	9.45
PD1468	<i>bolA</i>	Morphogene BolA protein	236.76	2,306.64	9.74
PD1392	<i>gumF</i>	GumF protein	13.10	233.62	17.83
PD1222		Hypothetical protein	321.58	12,183.51	37.89
PD0657		Hypothetical protein	70.31	2,857.66	40.65
PD0215	<i>cvaC</i>	Colicin V precursor	1,211.81	105,871.34	87.37

absence of pili. Several differentially expressed genes encoding proteins directly involved in attachment, motility, and/or biofilm formation included *pilA1* (PD1924), *pilA2* (PD1926), *fimA* (PD0062), *fimC* (PD0061), *hsf/xadA* (PD0824), *pilV* (PD0020), and *fimT* (PD1735). We performed quantitative reverse transcriptase PCR (qRT-PCR) for several of these genes and saw that expression of *pilA1* was consistently upregulated in the *csp1* mutant strain in multiple independent replicates of qPCR using RNA extracted separately from *X. fastidiosa* cells grown under the same conditions (Table 2). We also observed differential expression of several genes encoding ribosomal components that have previously been associated with biofilm growth (as opposed to planktonic cell growth) (21). It is likely that differential expression of ribosomal components in the  $\Delta csp1$  mutant is related to the difference in biofilm development in this mutant as well, but further experiments were focused on *pilA1* because of the deficiency in pili formation in  $\Delta csp1$ .

**Stag's Leap  $\Delta pilA1$  mutant showed increased biofilm formation and decreased cellular aggregation *in vitro*.** *X. fastidiosa* PilA1 is a type IV pili subunit protein that contributes to biofilm formation (22). Studies in *X. fastidiosa* strains TemeculaL and WM1-1 showed that deleting *pilA1* leads to overabundance of type IV pili and increased attachment and biofilm formation (22). We observed increased expression of *pilA1*, decreased cell-to-cell

**TABLE 2** Quantitative RT-PCR results for *pilA1* expression

Gene	Relative normalized expression of:		
	WT	$\Delta csp1$	$\Delta csp1+$
<i>pilA1</i>	1.00	7.29 $\pm$ 4.35	0.50 $\pm$ 0.36

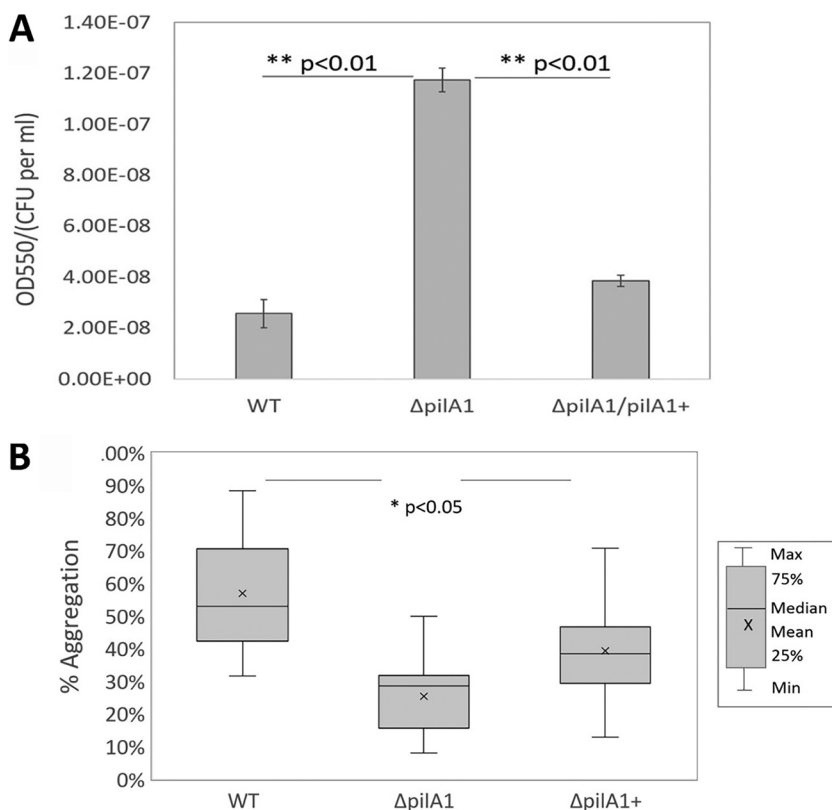


**FIG 4** Cellular aggregation and attachment of  $\Delta pilA1$ . (A) Cell attachment of wild-type Stag's Leap (WT),  $pilA1$  deletion mutant ( $\Delta pilA1$ ), and  $pilA1$  complemented strain ( $\Delta pilA1/pilA1+$ ) was quantified by measuring the amount of crystal violet stain retained by cells attached to the walls of 15-ml polystyrene culture tubes (OD<sub>550</sub>) after static growth in 5 ml of PD3 liquid medium for 7 days. OD<sub>550</sub> was normalized to total cells (CFU per ml) quantified by qPCR. Graph represents at least 16 technical replicates from four separate experiments. \*\*, significant difference from wild type based on one-way ANOVA followed by Tukey means comparison test ( $P < 0.01$ ). (B) Cellular aggregation was quantified by measuring the OD<sub>600</sub> of statically grown liquid cultures of WT,  $\Delta pilA1$ , and  $\Delta pilA1/pilA1+$  before and after manual dispersal of cells. The percentage of aggregated cells was calculated using the equation from Figure 2B. The graph represents a total of at least 9 technical replicates from three separate experiments. \*, significant difference based on one-way ANOVA followed by Tukey means comparison test ( $P < 0.05$ ).

adhesion, and decreased attachment to surfaces in the Stag's Leap  $\Delta csp1$  mutant, so we created a  $pilA1$  deletion mutant in the Stag's Leap background to further investigate the role of  $pilA1$  expression in the phenotypes observed in  $\Delta csp1$ . Like TemeculaL, the Stag's Leap  $\Delta pilA1$  strain showed an increase in surface attachment compared to that of the wild type and complemented strains (Fig. 4A). The  $\Delta pilA1$  mutant also had reduced cellular aggregation and a dispersed phenotype in liquid media (Fig. 4B). TEM images of Stag's Leap  $\Delta pilA1$  show that, like deleting the TemeculaL  $\Delta pilA1$  mutant, deleting  $pilA1$  in Stag's Leap also leads to overabundance of pili distributed around the entire cell (Fig. S3). These results show that  $pilA1$  is important for attachment and biofilm formation in Stag's Leap and suggest that the decrease in surface attachment observed in the  $\Delta csp1$  mutant may be a result of increased expression of  $pilA1$ .

**The  $\Delta pilA1$  mutant showed reduced virulence in grapevines.** Xylem vessel occlusion caused by biofilms is one major mechanism of *X. fastidiosa* pathogenicity. Previous studies showed that the  $\Delta csp1$  mutant is less virulent in Chardonnay grapevines compared to wild-type Stag's Leap (16). Since both the  $\Delta csp1$  and  $\Delta pilA1$  mutant strains have altered biofilm phenotypes, and  $pilA1$  expression is upregulated in the  $\Delta csp1$  strain, we were interested to see if  $pilA1$  also influences virulence in grapevines. We inoculated susceptible 1-year-old potted Chardonnay grapevines with wild-type

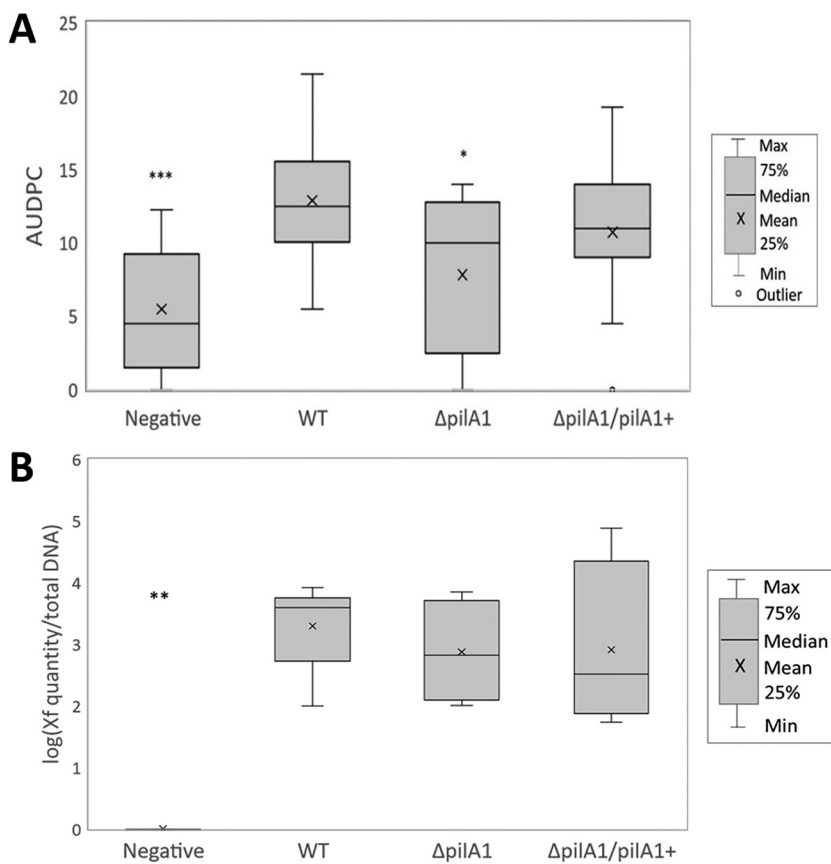


**FIG 5**  $\Delta pilA1$  has reduced symptom development in grapevines. One-year-old potted grapevines (cv. Chardonnay) were mechanically inoculated with wild-type Stag's Leap (WT), *pilA1* deletion mutant ( $\Delta pilA1$ ), the complemented ( $\Delta pilA1/pilA1+$ ) strain, or 1× PBS as the negative control. (A) Symptom development in grapevines was scored on a 0 to 5 scale, with 0 indicating no symptoms and 5 indicating plant death, over the period of 5 to 16 weeks postinoculation. Area under the disease progress curve (AUDPC) was calculated using the Agricolae package for R. (B) Bacterial populations in plant tissue were quantified using qPCR after 16 weeks postinoculation and normalized to total DNA concentration. Graphs represents data from 20 plants inoculated with wild type, 15 plants inoculated with  $\Delta pilA1$ , 15 plants inoculated with  $\Delta pilA1/pilA1+$ , and 10 negative-control plants. \*, treatment significantly different from the wild type based on one-way ANOVA followed by Tukey means comparison test (\*,  $P < 0.05$ ; \*\*,  $P < 0.01$ ; \*\*\*,  $P < 0.001$ ).

Stag's Leap,  $\Delta pilA1$ , and  $\Delta pilA1/pilA1+$  cultures or 1× phosphate-buffered saline (PBS) as the negative control. Disease ratings were assessed using the grapevine symptom rating scale (23) (Fig. S2). Disease severity was significantly reduced for plants inoculated with the  $\Delta pilA1$  strain compared with that for plants inoculated with wild-type and complemented strains at 16 weeks postinoculation (Fig. 5A). The bacterial populations in inoculated plants were also quantified using quantitative PCR (qPCR). There was no significant difference in *X. fastidiosa* populations detected in petioles from plants inoculated with  $\Delta pilA1$ , wild type, or the complemented strains at 16 weeks postinoculation (Fig. 5B). This suggests that the virulence defect of the mutant strain was not due to reduced bacterial populations.

## DISCUSSION

In this study, we explored the role of Csp1 and biofilm-related gene expression in bacterial plant pathogen *X. fastidiosa*. Deleting the *csp1* gene in strain Stag's Leap influenced expression of 90 genes, several of which encode proteins related to bacteria attachment and motility. The phenotype of the  $\Delta csp1$  mutant supported our transcriptome data, showing changes in cellular aggregation and surface attachment, processes

that involve type I and type IV pili (20, 24). TEM images of  $\Delta csp1$  showed a significant reduction in the number of visible pili compared to that in the wild-type and complemented strains. Deleting *csp1* also reduced bacterial viability during late stationary phase, suggesting that Csp1 is important for long-term survival.

Biofilm formation is an important part of *X. fastidiosa* insect vector and plant colonization (25). Xylem blockage by biofilms restricts water flow and is a major mechanism of *X. fastidiosa* pathogenicity (26). Biofilm development in *X. fastidiosa* is highly regulated and requires surface attachment and cellular aggregation, which are dependent on type I and type IV pili (27). Our RNA-Seq data showed upregulation of the type IV pili gene *pilA1* in the  $\Delta csp1$  mutant. When *pilA1* was deleted from the Stag's Leap genome, we observed increased surface attachment and decreased cellular aggregation. Electron microscopy of the Stag's Leap, TemeculaL (22), and WM1-1 (22)  $\Delta pilA1$  mutants showed increased pili abundance with pili distributed around the entire cell, unlike their respective wild-type strains, which showed only pili localized to one cell pole. In contrast, the  $\Delta csp1$  mutant, which showed upregulation of *pilA1*, appears to be deficient in pili formation compared to wild-type Stag's Leap. The lack of visible pili in  $\Delta csp1$  may contribute to the reduced attachment phenotype observed for this strain, while the increased abundance of type IV pili in the  $\Delta pilA1$  mutants may contribute to increased attachment. Differential expression of other biofilm-related genes includes downregulation of type IV pili genes *pilA2* (PD1926) and *fimT* (PD1735) and type I pilin gene *fimA* (PD0062) in the  $\Delta csp1$  strain. Previous studies showed that *X. fastidiosa* mutants lacking *fimA* had aggregation- and biofilm-deficient phenotypes but were twitching enhanced (24, 28), while mutants in *pilA2* were twitching deficient compared to the wild type (22). Twitching motility allows *X. fastidiosa* to move against xylem flow and colonize tissue beyond the point of inoculation, making it important for virulence and plant colonization (29). Twitching motility of the  $\Delta csp1$  mutant was not examined in this study but would be of interest for future studies to elucidate whether Csp1 influences this type of movement in *X. fastidiosa* and whether it contributes to virulence and bacterial titer in grapevines. In addition, future experiments investigating *in planta* biofilm formation of the  $\Delta csp1$  mutant can give us a better understanding of how Csp1 influences *X. fastidiosa* plant colonization.

We also observed downregulation of *gacA* in  $\Delta csp1$ , which encodes a response regulator that influences expression of genes related to attachment and biofilm formation in *X. fastidiosa* (30). In *X. fastidiosa* A05, a *gacA* mutant strain was deficient in cell-to-cell aggregation and surface attachment and showed differential expression of 27 genes (30), including similar regulation in several genes that were also differentially expressed in our  $\Delta csp1$  mutant. These shared genes of interest include downregulation of *cvaC* (PD0216) and *pilA2* and upregulation of *cvaC* (PD0215) and four hypothetical proteins (PD1702, PD1703, PD0521, PD0657) (30). The *hsf* (PD0744) gene encoding a surface protein was downregulated in the *gacA* mutant (30) but was upregulated in our  $\Delta csp1$  mutant. The *gacA* *X. fastidiosa* mutant study did not show differential expression of *csp1*, *pilA1*, or some of the other genes encoding pili components that were differentially expressed in our study. These results suggest that the influence of Csp1 on *gacA* expression may also contribute to the attachment and aggregation phenotypes we observed in the  $\Delta csp1$  Stag's Leap mutant but that *csp1* may be higher up in the biofilm gene regulation network. Future studies looking at the relationship between Csp1 and *gacA* expression can shed light on regulatory networks in *X. fastidiosa*.

Our Stag's Leap  $\Delta pilA1$  mutant was also less virulent in susceptible Chardonnay grapevines. *X. fastidiosa* disease symptom development is strongly correlated with pathogen spread within infected plants (20, 29), so increased surface attachment of the  $\Delta pilA1$  mutant may restrict bacterial spread within the xylem, leading to the reduced virulence phenotype observed. However, there was no significant difference in bacterial titer between  $\Delta pilA1$  and the wild-type or complemented strains, suggesting that the virulence defect of  $\Delta pilA1$  may not be entirely due to reduced colonization. The  $\Delta csp1$  mutant showed

upregulation of *pilA1* and decreased virulence in grapevines, while the  $\Delta$ *pilA1* mutant also had reduced virulence in grapevines, indicating that other factors besides increased expression of *pilA1* are contributing to the Csp1-related virulence defect. Other variables that may affect virulence include decreased expression of virulence regulators (PD1905/*xrvA* and PD0708) in  $\Delta$ *csp1*. The functions of XrvA and the putative PD0708 protein in *X. fastidiosa* are still unclear. In *Xanthomonas oryzae* pv. *oryzae*, the *xrvA* gene encodes a protein containing a histone-like nucleoid-structuring protein (H-NS) domain and a mutation in *xrvA* resulted in reduced virulence in rice host plants (31). Future studies investigating the functions of XrvA in *X. fastidiosa* can shed light on its potential role virulence.

The Stag's Leap  $\Delta$ *csp1* mutant was less viable at 13 days postinoculation, which is considered the late stationary phase of growth for this strain of *X. fastidiosa*, compared to the wild-type and complemented strains. Bacteria in stationary phase encounter many stressors, including nutrient limitation, accumulation of toxic byproducts, and changes in pH, temperature, osmolarity, etc. (32). Studies in other bacteria show that several temperature-independent cold shock proteins are involved in stationary-phase stress response. *E. coli* CspD, which is 55.2% identical to the *X. fastidiosa* Csp1 amino acid sequence, is expressed during stationary phase upon glucose starvation and oxidative stress (15). The function of CspD is inhibition of DNA replication by nonspecific binding to single-stranded DNA regions at replication forks (33), and deletion of *cspD* leads to decreased persister cell formation, while overexpression of *cspD* is lethal in *E. coli* (33). Bacterial persister cells are more resistant to antibiotics and can often be found in biofilm communities (34). Bacteria in biofilms are more resistant to host defense responses and antimicrobial compounds (35, 36) and have increased nutrient availability (37). Copper-based products are often used to control bacterial pathogens in agriculture, and transcriptome studies show that treating *X. fastidiosa* subsp. *pauca* biofilms with copper resulted in upregulation of genes important for biofilm and persister cell formation, including the toxin-antitoxin system MqsR/MqsA (38) which, in *E. coli*, regulates expression of *cspD*. The *E. coli* MqsR toxin is also directly involved in biofilm development and is linked to the development of persister cells (38). Overexpression of the *X. fastidiosa* MqsR toxin in a citrus pathogenic strain led to increased biofilm formation and decreased cell movement, resulting in reduced pathogenicity in citrus plants. In *X. fastidiosa* Temecula-1, an *mqsR* deletion mutant had reduced biofilm formation (39). MqsR overproduction also increased persister cell formation under copper stress in *X. fastidiosa* (40). It is unknown whether *csp1* expression in Stag's Leap is regulated or influenced by the MqsR/MqsA complex; however, functional similarities between Csp1 and CspD and the results from studies in *E. coli* showing that *cspD* is directly regulated by MqsR/MqsA suggest that this is a possibility. Future studies looking at possible links between Csp1 and the MqsR/MqsA toxin-antitoxin system can shed more light on *X. fastidiosa* stress tolerance and survival.

In summary, our study showed novel findings that a cold shock protein homolog in *X. fastidiosa* influences gene expression and biofilm-related phenotypes. Biofilm formation is an essential virulence factor for *X. fastidiosa* and also contributes to bacterial stress tolerance. The results of this study highlight the complexity of *X. fastidiosa* pathogen biology, and more work looking at how cold shock proteins affect these processes will help us better understand how this pathogen colonizes and causes disease in hosts.

## MATERIALS AND METHODS

**Bacterial culture conditions.** The wild-type strain used in this study is *Xylella fastidiosa* subspecies *fastidiosa* strain Stag's Leap isolated from grapevines with Pierce's disease in California, USA (41). The  $\Delta$ *csp1* mutant strain used in this study has the *csp1* (PD1380) gene deleted and replaced with a chloramphenicol resistance cassette (16). For all *in vitro* experiments, *X. fastidiosa* strains were grown on PD3 (42) agar plates or liquid PD3 medium without antibiotics or supplemented with 5  $\mu$ g/ml of chloramphenicol and/or gentamicin when needed. *Escherichia coli* strains used for cloning and propagating of plasmid constructs were grown on LB medium supplemented with appropriate antibiotics at the following concentrations: chloramphenicol 35  $\mu$ g/ml, spectinomycin 100  $\mu$ g/ml, and gentamicin 10  $\mu$ g/ml. All bacterial strains and plasmids used in this study are listed in Table 2 and 3, respectively.

**TABLE 3** Bacteria strains

Strain	Description	Source
<i>Xylella fastidiosa</i>		
Subspecies <i>fastidiosa</i> Stag's Leap	Wild-type strain, used to create mutant	41
$\Delta csp1$	<i>X. fastidiosa</i> deletion mutant in <i>csp1</i> (PD1380), Cm <sup>R</sup>	16
$\Delta csp1/csp1+$	Complemented strain, constructed by chromosomal insertion of <i>csp1</i> ORF at neutral site, Cm <sup>R</sup> , Gm <sup>R</sup>	16
$\Delta pilA1$	<i>X. fastidiosa</i> deletion mutant in <i>pilA1</i> (PD1924), Cm <sup>R</sup>	This study
$\Delta pilA1/pilA1+$	Complemented strain, constructed by chromosomal insertion of <i>pilA1</i> ORF at neutral site, Cm <sup>R</sup> , Gm <sup>R</sup>	This study
One Shot TOP10 chemically competent <i>E. coli</i>	Commercially available <i>E. coli</i> strain used for propagating plasmid constructs, genotype: F- <i>mcrA</i> $\Delta$ ( <i>mrr-hsdRMS-mcrBC</i> ) $\Phi$ 80 <i>lacZ</i> $\Delta$ M15 $\Delta$ <i>lacX74recA1 araD139 <math>\Delta</math>(<i>araleu</i>)7697 <i>galU galK rpsL</i> (StrR) <i>endA1 nupG</i></i>	Invitrogen

**Construction of mutant and complemented strains.** The *X. fastidiosa*  $\Delta pilA1$  mutant strain was constructed by replacing the *pilA1* open reading frame with the chloramphenicol resistance cassette from plasmid pCR8-*csp1*-chl (16) using homologous recombination. Homologous recombination in *X. fastidiosa* is highly efficient, and none of the plasmids used for transformation can replicate in this species. A total of 931 bp of the upstream flanking region of the *pilA1* coding sequence were amplified from the WT Stag's Leap genomic DNA (gDNA) using the primers *pilA1*-up-F/*pilA1*-up-R-SacI (Table 4). The *pilA1*-up-R-SacI adds a SacI restriction site to the 3' end of the PCR product. A total of 1.3 kb of the downstream flanking region of the *pilA1* coding sequence were amplified using primers *pilA1*-down-F-XbaI/*pilA1*-down-R (Table 4). The *pilA1*-down-F-XbaI primer adds the XbaI restriction site to the 5' end of the PCR product. The chloramphenicol resistance cassette from pCR8-*csp1*-chl (16) was amplified using primers Chl-F-SacI/Chl-R-XbaI, which add SacI and XbaI restriction sites to the 5' and 3' ends, respectively, of the chloramphenicol resistance cassette amplicon. All PCRs were performed using the high-fidelity Platinum *Taq* DNA polymerase (Thermo Fisher). The chloramphenicol resistance cassette amplicon was ligated to the *pilA1* upstream and downstream flanking region amplicons using restriction cloning with SacI and XbaI (New England Biolabs) and T4 DNA ligase (Invitrogen). The ~3.5-kb ligation product was cloned into rapid TA cloning vector pCR8/GW/TOPO (Thermo Fisher) following the manufacturer's instructions to create pCR8- $\Delta pilA1$ -chl. The TA cloning reaction was transformed into *E. coli* OneShot Top 10 competent cells (Thermo Fisher) and cells were spread onto LB agar supplemented with 100  $\mu$ g/ml spectinomycin for selection of transformants. Transformants were screened for the correct 3.5-kb insert using colony PCR with the primers *pilA1*-up-F/*pilA1*-down-R. Five colonies with the correct-sized insert were inoculated into liquid LB supplemented with spectinomycin and chloramphenicol and grown overnight at 37°C for plasmid extraction using a QIAprep Spin miniprep kit (Qiagen). The plasmid constructs were confirmed by Sanger sequencing. Plasmid pCR8- $\Delta pilA1$ -chl was then transformed into WT *X. fastidiosa* using the natural transformation protocol (43) for mutagenesis via homologous recombination. Transformants were selected on PD3 agar supplemented with chloramphenicol, and resistant colonies were screened by colony PCR using *X. fastidiosa*-specific primers RST31/RST33 (44) and gene-specific primers to confirm the size of the insertion region (*pilA1*-ORF-F/*pilA1*-ORF-R; Table 4). The deletion mutation was confirmed by Sanger sequencing of the recombination region.

For complementation of the *pilA1* deletion, the *pilA1* open reading frame (ORF) plus upstream and downstream flanking regions was inserted into the chromosome of the *X. fastidiosa*  $\Delta pilA1$  strain at a neutral site as described previously (45). The *pilA1* ORF plus 405 bp of upstream and 215 bp of downstream sequence was PCR amplified from WT Stag's Leap gDNA template using Platinum *Taq* polymerase and primers *pilA1*-ORF-405-F/*pilA1*-ORF-R (Table 4) and TA cloned into pCR8/GW/TOPO to create pCR8-*pilA1*-ORF (Table 3). Plasmid pCR8-*pilA1*-ORF was recombined with plasmid pAX1-GW (16) (Table 3) using the Gateway LR recombination protocol (Invitrogen). The resulting plasmid, pAX1-*pilA1*-ORF, was purified from *E. coli* transformants and the correct insertion was confirmed by Sanger sequencing. pAX1-*pilA1*-ORF was naturally transformed into the *X. fastidiosa*  $\Delta pilA1$  strain, and transformants

**TABLE 4** Plasmids

Plasmid	Description	Source
pCR8/GW/TOPO	Commercially available cloning vector with 3'-T overhangs. Compatible with Gateway destination vectors, Sp <sup>R</sup>	Invitrogen
pCR8- $\Delta pilA1$ -chl	<i>pilA1</i> gene deletion construct containing chloramphenicol resistance marker flanked by ~1.5 kb upstream and downstream sequences of <i>pilA1</i> gene, <i>pilA1</i> ORF is deleted, Sp <sup>R</sup> , Cm <sup>R</sup>	This study
pCR8- <i>pilA1</i> -ORF	<i>pilA1</i> complementation construct containing the <i>X. fastidiosa</i> <i>pilA1</i> ORF and flanking regions. Used with Gateway pAX1-GW destination vector, Sp <sup>R</sup>	This study
pAX1-GW	Gateway destination vector used for <i>Xf</i> chromosomal gene complementation into neutral location via homologous recombination, Cm <sup>R</sup> , Gm <sup>R</sup>	45
pAX1- <i>pilA1</i> -ORF	Gateway complementation construct with ORF of <i>Xf pilA1</i> and flanking regions, Gm <sup>R</sup>	This study

were selected on PD3 agar plates supplemented with gentamicin. Transformants were screened using colony PCR with *X. fastidiosa*-specific primers (RST31/RST33) and gene-specific primers (pilA1-ORF-405-F/pilA1-ORF-R). Correct insertion of complementation constructs was confirmed by Sanger sequencing.

**Cell aggregation assay.** *X. fastidiosa* strains were grown on PD3 agar plates and incubated at 28°C for 6 to 7 days. After incubation, bacterial cells were scraped off plates and resuspended in 5 ml of liquid PD3 medium (per sample) to an optical density at 600 nm ( $OD_{600}$ ) of 0.10. Liquid cultures were grown in sterile 15-ml polypropylene test tubes at 28°C without shaking for 6 to 7 days. At least 3 replicates per strain were included. Cell aggregation was quantified using the  $OD_{600}$  of the upper culture (ODs) and the  $OD_{600}$  of the total culture ( $OD_T$ ). ODs, which is composed mostly of dispersed cells, was determined by measuring  $OD_{600}$  of undisturbed cultures.  $OD_T$  was measured after aggregated cells were dispersed using a pipette and vortexed. The relative percentage of aggregated cells was estimated using the formula  $[(OD_T - OD_s)/OD_T] \times 100$  (46). The assay was repeated at least three separate times.

**Cell attachment assay.** All procedures for setting up the attachment assays were performed aseptically. *X. fastidiosa* strains used in the attachment assays were grown on PD3 agar plates and incubated at 28°C for 6 to 7 days. After incubation, bacterial cells were scraped off plates and resuspended in 1 ml (per sample) of liquid PD3 medium. Small volumes of the concentrated cell suspensions were pipetted into 5 ml (per sample) of fresh PD3 medium until a concentration of  $OD_{600}$  of 0.03 to 0.05 was reached. Aliquots of 100  $\mu$ l of cell suspensions were added to individual wells of sterile 96-well polystyrene plates with lids (Nunc, catalog no. 163320). Of the remaining cell suspension, 1 ml of each sample was transferred into sterile 1.5-ml centrifuge tubes and incubated at 28°C for 4 days (for gDNA extraction and qPCR later). Uninoculated liquid PD3 medium was used as a negative control. To minimize evaporation issues, we did not use wells from the outermost rows and columns of the plates. Plates were double wrapped with parafilm and incubated at 28°C for 4 days. Cell attachment was quantified using crystal violet staining. Medium was removed from 96-well plates and the wells were washed three times with distilled water to remove unbound (planktonic) cells. Cells adhering to the sides of individual wells were stained with 100  $\mu$ l of 0.1% (wt/vol) crystal violet for 25 min at room temperature. Crystal violet solution was removed from wells and wells were washed three times with distilled water. Crystal violet stain retained by attached cells was eluted by adding 100  $\mu$ l of 30% acetic acid (47) to each well and quantified using a microplate reader (Tecan Infinite M1000 PRO) at 550 nm wavelength.  $OD_{550}$  results were normalized to CFU/ml of cells determined by qPCR. For qPCR, 1-ml aliquots of cells were centrifuged at 9,000 rpm for 3 min to pellet cells and then frozen at  $-20^\circ\text{C}$  until DNA extraction. DNA extraction was performed using a DNeasy blood and tissue kit (Qiagen) following the manufacturer's protocol for Gram-negative bacteria. DNA was resuspended in 50  $\mu$ l of sterile diethylpyrocarbonate (DEPC) water (Invitrogen). One microliter of each DNA sample was used as the template for qPCR with Applied Biosystems PowerUp SYBR green master mix (Thermo Fisher) and primers targeting the *X. fastidiosa* chromosome (XfITS145-60F/XfITS145-60R; Table 4). Concentration in CFU/ml was determined based on a standard curve of *X. fastidiosa* DNA extracted from samples with known CFU/ml concentrations. Cell attachment assays were repeated three separate times.

**Cell viability assay.** Wild type,  $\Delta csp1$ , and  $\Delta csp1/csp1+$  strains were grown on PD3 agar plates for 7 to 13 days at 28°C. Cells were scraped off plates and resuspended in  $1 \times$  PBS and diluted to an  $OD_{600}$  of 0.01. One-milliliter aliquots of each sample were reserved for gDNA extraction for cell quantification by qPCR. Ninety microliters of cell suspensions was added to individual wells of sterile 96-well plates and 10  $\mu$ l of alamarBlue cell viability reagent (Invitrogen) was mixed into each well. Plates were incubated in the dark at 37°C for 2 h. Fluorescence was measured at 560 nm excitation/590 nm emission using a Tecan Infinite M1000 Pro plate reader. Cell aliquots reserved for qPCR were centrifuged at max speed for 3 min to pellet cells and then frozen at  $-20^\circ\text{C}$  until DNA extraction. DNA extraction was performed using a DNeasy blood and tissue kit (Qiagen) following the manufacturer's protocol for Gram-negative bacteria. DNA was resuspended in 50  $\mu$ l of distilled water ( $\text{dH}_2\text{O}$ ). One microliter of each DNA sample was used as the template for qPCR with Applied Biosystems PowerUp SYBR green master mix (Thermo Fisher) and primers targeting the *X. fastidiosa* chromosome (XfITS145-60F/XfITS145-60R; Table 4). Concentration in CFU/ml was determined based on a standard curve of *X. fastidiosa* DNA extracted from samples with known CFU/ml concentrations. Fluorescence readings were normalized to CFU/ml.

**Transmission electron microscopy of *X. fastidiosa*.** *X. fastidiosa* cells were grown on modified periwinkle wilt (PW) agar (omit phenol red and add 1.8 g/liter of bovine serum albumin) (22) for two to 3 days. We placed 3 mm 300 mesh TEM grids directly on bacterial cells growing on agar medium for 5 s. Grids were immediately placed on a drop of 1.0% phosphotungstic acid for 30 s. Excess stain was wicked off the grid and placed in the FEI Helios Nanolab 650 SEM for STEM imaging. TEM was performed by Teresa Sawyer at the Oregon State University Electron Microscopy Facility (Corvallis, OR).

**RNA-Seq analysis. Bacteria growth conditions.** WT Stag's Leap and  $\Delta csp1$  strains were grown on PD3 agar plates for 6 days at 28°C (6 plates per strain). Cells were aseptically harvested from each plate for all strains and immediately frozen on dry ice for RNA extraction later. Three replicates were included per strain, and each replicate sample included cells from two separate plates.

**RNA preparation.** Total bacterial RNA was extracted from frozen cells using the TRIzol extraction method as described. Briefly, 1 ml of TRIzol (Invitrogen) reagent was added to each sample (in 1.5-ml centrifuge tubes) and incubated at room temperature for 5 min. Samples were centrifuged to remove debris and the supernatant was transferred into new 1.5-ml tubes. A total of 0.2 ml of chloroform was added to each sample and mixed thoroughly. Samples were centrifuged at  $12,000 \times g$  for 15 min. Following centrifugation, the colorless upper aqueous phase containing the RNA was transferred into a fresh tube and RNA was precipitated by adding 0.5 ml of room temperature isopropyl alcohol. Samples were incubated at room temperature for 10 min and centrifuged at  $12,000 \times g$  for 10 min. The RNA

pellet was washed twice with 1 ml of 75% ethanol. Ethanol was removed and the RNA pellet was air dried and dissolved in DEPC-treated water. Total RNA was quantified using Quant-iT RNA assay kit (Invitrogen). Five micrograms of total RNA was treated with DNase I (Thermo Fisher) following the manufacturer's protocol. DNase-treated RNA was reprecipitated using 0.1 volume sodium acetate and 3× volume ethanol. Poly(A) tail was added to the bacterial mRNA using poly(A) tailing kit (Invitrogen) following the manufacturer's protocol. RNA was reprecipitated using sodium acetate and resuspended in DEPC water (Tris-EDTA [TE] buffer was not used because EDTA concentrations as low as 1 mM will inhibit activity of exonuclease used in the next step). rRNA was removed using the Lucigen terminator 5'-phosphate-dependent exonuclease kit following the manufacturer's protocol. The reaction was terminated, and the remaining RNA was precipitated using sodium acetate and ethanol. RNA quantity and quality were measured on the Agilent bioanalyzer 2100 prior to cDNA library synthesis.

**Nanopore cDNA library preparation.** cDNA library synthesis was performed using the Oxford nanopore direct cDNA synthesis kit (Oxford Nanopore) following the manufacturer's protocol. All cDNA synthesis-specific reagents and consumables used were included in the kit unless stated otherwise. A total of 250 ng of PolyA+ mRNA resuspended in 7.5  $\mu$ l of nuclease-free water (per sample) was added to DNA LoBind tubes and centrifuged briefly. Reverse transcription and strand-switching were performed by first adding 2.5  $\mu$ l VNP primer and 1  $\mu$ l 10 mM deoxynucleoside triphosphates (dNTPs) (ThermoFisher) to each mRNA sample and incubating at 65°C for 5 min, followed by immediately cooling on ice. In separate tubes, 4  $\mu$ l of 5× Maxima H Minus RT buffer (Thermo Fisher), 1  $\mu$ l RNaseOUT (Thermo Fisher), 1  $\mu$ l nuclease-free water, and 2  $\mu$ l strand-switching primer (SSP) were combined and added to the mRNA samples. Samples were incubated at 42°C for 2 min, after which 1  $\mu$ l of Maxima H Minus reverse transcriptase (Thermo Fisher) was added to each sample. Samples were incubated at 42°C for 90 min, followed by heat inactivation of reaction at 85°C for 5 min. Residual RNA was digested by adding 1  $\mu$ l of RNase cocktail enzyme mix (Thermo Fisher) to each reverse transcription reaction. Samples were transferred to new 1.5-ml DNA LoBind Eppendorf tubes and cDNA was purified using 17  $\mu$ l of resuspended AMPure XP beads (Agencourt) following the manufacturer's protocols. Samples mixed with AMPure XP beads were centrifuged briefly and beads (bound to cDNA) were immobilized to tube walls using a magnetic tube rack. Tubes were kept on the magnetic rack and the supernatant was removed and discarded. The beads were washed twice with 200  $\mu$ l freshly prepared 70% molecular grade ethanol. Residual ethanol was removed, and bead pellets were air dried briefly (not to the point of the pellet cracking). Tubes were removed from the magnetic rack and bead pellets were resuspended in 20  $\mu$ l of DEPC water (Invitrogen). Tubes were put back on the magnetic rack to separate the eluate from the AMPure XP beads, and 20  $\mu$ l of eluate from each sample was transferred into separate 0.2-ml PCR tubes for cDNA second strand synthesis. A total of 25  $\mu$ l 2× LongAmp Taq master mix (New England Biolabs), 2  $\mu$ l PR2 primer, and 3  $\mu$ l of DEPC water was added to each 20- $\mu$ l eluate sample. Thermal cycler conditions were as follows: 94°C for 1 min, 50°C for 1 min, 65°C for 15 min, hold at 4°C until next step. Samples were transferred into 1.5-ml DNA LoBind tubes and cDNA was purified using 40  $\mu$ l of AMPure XP beads following the same protocol as that described previously. Purified cDNA was eluted in 21  $\mu$ l of DEPC water. One microliter of purified cDNA was analyzed on the Agilent Bioanalyzer 2100 to check the quality and quantity. End repair and dA-tailing of fragmented cDNA were performed by mixing 20  $\mu$ l cDNA sample, 30  $\mu$ l nuclease-free water, 7  $\mu$ l Ultra II end-prep reaction buffer (New England Biolabs), and 3  $\mu$ l Ultra II end-prep enzyme mix (New England Biolabs). Samples were incubated at 20°C for 5 min, followed by 65°C for 5 min in a thermal cycler. Samples were transferred into 1.5-ml DNA LoBind Eppendorf tubes and purified using 60  $\mu$ l of AMPure XP beads following the same protocol as before. Samples were resuspended in 22.5  $\mu$ l of DEPC water and transferred into clean 1.5-ml Eppendorf DNA LoBind tubes.

**Barcode ligation.** Individual cDNA libraries (12 total) were ligated with unique native barcodes (Oxford nanopore native barcode expansion sets 1 to 12) following the manufacturer's protocols. A total of 22.5  $\mu$ l of cDNA was combined with 2.5  $\mu$ l native barcode and 25  $\mu$ l Blunt/TA ligase master mix (New England Biolabs). Samples were incubated at room temperature for 10 min, and barcoded cDNA libraries were purified using 40  $\mu$ l of AMPure XP beads and resuspended in 26  $\mu$ l DEPC water following the same protocol as that used during cDNA library preparation. One microliter of each sample was quantified using the Quant-iT high-sensitivity dsDNA assay kit (Thermo Fisher). The quantity of cDNA for one replicate sample of WT 28°C was too low and was excluded from further experiments. The barcoded cDNA libraries from the remaining 11 samples were pooled in equal ratios to obtain 700 ng total DNA and final volume adjusted to 50  $\mu$ l using nuclease-free water and loaded into the Nanopore MinION flow cell (FLO-MIN106). The sequencing reaction was run for 23 h and generated approximately 4.04 million total reads in FAST5 format.

**Data analysis.** Nanopore FAST5 files were converted into FASTQ files using the basecalling program Guppy (48). Barcoded samples were demultiplexed using Deepbinner (49). The program Porechop was used to trim off adapter sequences from the demultiplexed FASTQ reads. The *X. fastidiosa* Temecula-1 cDNA reference transcriptome ([http://ftp.ensemblgenomes.org/pub/bacteria/release-44/fasta/bacteria\\_18\\_collection/xylella\\_fastidiosa\\_temecula1/cdna/](http://ftp.ensemblgenomes.org/pub/bacteria/release-44/fasta/bacteria_18_collection/xylella_fastidiosa_temecula1/cdna/)) was indexed and FASTQ reads were mapped to the reference using Minimap2 (50). After mapping, aligned reads were quantified using Salmon (51). A table summarizing transcript-level estimates for use in differential gene analysis was created using the R package tximport (52). Differential expression analysis was performed using the R package DESeq2 (53). Descriptions of the programs used and web addresses for downloading the source codes are listed in Table S1.

**qRT-PCR gene expression analysis.** Quantitative reverse transcriptase PCR (qRT-PCR) was used to look at gene expression results of several differentially expressed genes of interest from the RNA-Seq

TABLE 5 Primers

Primer name	Sequence 5'–3'	Source
RST31	GCGTTAATTTTCGAAGTGATTCGATTGC	44
RST33	CACCATTCTGATCCCGGTG	44
<i>pilA1</i> -up-F	GCCTTGCGAATTTTCCC	This study
<i>pilA1</i> -up-R-SacI	GGGGAGCTCGTGATACCTTCAATAAAAAGTTTGGT	This study
<i>pilA1</i> -down-F-XbaI	CCCTCTAGATGAATACACACAGCAACACGATCAATG	This study
<i>pilA1</i> -down-R	AATCGTGTTGTTGCTGGTG	This study
<i>pilA1</i> -ORF-405F	CCGCAGTACGTGTTGC	This study
<i>pilA1</i> -ORF-R	GTTGTAACGGCTCACTC	This study
XfITS145-60F	TACATCGGAATCTACCTTATCGTG	55
XfITS145-60R	ATGCGGTATTTAGCGTAAGTTTC	55
<i>csp1</i> -qPCR-F	TGATGGGACTCCCGAGGTAT	16
<i>csp1</i> -qPCR-R	GGCCTTCATGCAAACACTACGG	16
PD1924-qRT-F ( <i>pilA1</i> )	TATGTTGCCAGATCCCAAGTC	This study
PD1924-qRT-R ( <i>pilA1</i> )	TCACCTGAGAATTGCCCTTAAT	This study
<i>dnaQ</i> -qPCR-F	CGTTATCCGGGTCAGCGTAA	54
<i>dnaQ</i> -qPCR-R	GTAACCTGACGGTGGGCGTTA	54

experiment, as well as to monitor expression of *csp1* during different *X. fastidiosa* growth stages. For RNA extraction for differentially expressed genes of interest, cells were grown under the same conditions as for the RNA-Seq experiment. For *csp1* expression, cells were grown as described in the cell viability assay. Total RNA was extracted as described in the RNA-Seq methods section using the TRIzol (Invitrogen) method. gDNA was removed using Baseline Zero DNase (Lucigen) following the manufacturer's protocols and RNA reprecipitated using 0.1 volume of sodium acetate and 2 to 3 volumes 100% ethanol. Purified RNA was quantified using a Quant-IT RNA assay kit (Thermo Fisher Scientific). Removal of residual DNA was confirmed by DNA-specific quantification using a Quant-IT dsDNA broad range assay kit (Thermo Fisher Scientific). For cDNA synthesis, 500 ng of total RNA was reverse transcribed with random primers using an iScript gClear cDNA synthesis kit (Bio-Rad) and including a no-RT and controls for each sample. One microliter of each cDNA sample was used as the template for qPCR using Applied Biosystems PowerUp SYBR green master mix (Thermo Fisher Scientific). *X. fastidiosa dnaQ* gene, which is a stable reference gene in *X. fastidiosa* (54), was used to normalize expression of other target genes. Relative normalized gene expression was calculated from the mean  $\pm$  standard deviation of at least 5 separate experiments after 30 cycles of qPCR. Primer sequences for target genes are listed in Table 5. PCR cycling conditions were based on recommended protocol provided by PowerUp SYBR green master mix and the melting temperature of the different primer sets. Experiments were repeated three independent times and relative gene expression was calculated with Bio-Rad CFX Manager software.

**Plant virulence assays. Plant inoculations.** Wild-type Stag's Leap,  $\Delta pilA1$ , and  $\Delta pilA1/pilA1+$  strains were grown on PD3 agar plates for 5 to 7 days and then scraped off plates and resuspended in  $1 \times$  PBS at a concentration of OD<sub>600</sub> of 0.25 ( $\sim 1 \times 10^8$  CFU/ml). Susceptible (cv. Chardonnay) 1-year-old potted grapevines were inoculated using a pinprick inoculation method (23). Mock inoculations using  $1 \times$  PBS were used as negative controls. Twenty plants were inoculated with wild type, 15 plants with  $\Delta pilA1$ , 15 plants with  $\Delta pilA1/pilA1+$ , and 10 plants with  $1 \times$  PBS. Plants were labeled with number codes and placed randomly within a climate-controlled greenhouse. The plants were monitored weekly for development of scorching symptoms. Once disease symptoms began to develop (5 weeks postinoculation for this experiment), plants were given a disease index score between 0 and 5 based on a rating scale developed previously (23). A disease score of 0 indicates no disease symptoms and a score of 5 represents severe disease symptoms and plant death. Representative images of disease ratings were provided courtesy of Yaneth Barreto-Zavala and are included in Figure S2. Plants were rated until 12 weeks postinoculation. Area under the disease progress curve (AUDPC) was calculated using average disease intensity over time (weeks) with the Agricolae package for R (<https://CRAN.R-project.org/package=agricolae>). Plant infection assays were conducted during June to September 2020.

**qPCR quantification of bacterial populations.** At 9 and 12 weeks postinoculation, petiole samples from infected and mock-inoculated plants were collected for DNA extraction and qPCR quantification of *in planta* bacterial populations. Two to three petiole samples from each plant were pooled, and samples were lyophilized using a FreeZone (LABCONCO) freezer dryer at  $-80^\circ\text{C}$  for 24 to 48 h. Lyophilized samples were pulverized with 3-mm tungsten carbide beads (Qiagen) using a Tissue Lyser II (Qiagen) for a total of 4 min at 30 rotations/second. One milliliter of DNA extraction buffer (20 mM EDTA, 350 mM Sorbitol, 100 mM Tris HCl) with 2.5% polyvinylpyrrolidone was added to each sample and centrifuged at 14,000 rpm for 5 min. All centrifugation steps were performed at  $4^\circ\text{C}$ . Supernatant was removed, and pellet was washed with an additional 1 ml of DNA extraction buffer and centrifuged for 10 min at 14,000 rpm. Supernatant was removed and pellet was resuspended with 300  $\mu\text{l}$  of DNA extraction buffer, 300  $\mu\text{l}$  of lysis buffer (50 mM EDTA, 2 M NaCl, 2% cetyltrimethylammonium bromide [CTAB], 200 mM Tris HCl), and 200  $\mu\text{l}$  of 5% sarcosyl. Tubes were incubated for 45 min at  $65^\circ\text{C}$  and mixed by vortexing every 15 min. After incubation, 700  $\mu\text{l}$  of chloroform/isoamyl alcohol (24:1) was added to each tube and inverted to mix samples. Samples were then centrifuged at 9,500 rpm for 5 min. The upper

phase was transferred to a new tube and 800  $\mu$ l of phenol/chloroform/isoamyl alcohol (25:24:1) was added. Samples were mixed and centrifuged at 9,500 rpm for 5 min. The upper phase was transferred to a new tube and 1 ml of isopropanol was added to precipitate the DNA. Samples were mixed and centrifuged at 12,000 rpm for 15 min. Supernatant was removed and pellet was washed with 300  $\mu$ l of chilled 70% ethanol and dried under a fume hood. DNA was then resuspended in 50  $\mu$ l of TE buffer. Samples were diluted 1:10 in sterile dH<sub>2</sub>O prior to quantification by qPCR.

For qPCR, 5  $\mu$ l of DNA was used as the template with Applied Biosystems Fast SYBR green master mix and primers targeting the *X. fastidiosa* chromosome (XfITS145-60F/XfITS145-60R; Table 4). A standard curve for quantification was made with 10-fold dilutions of *X. fastidiosa* DNA extracted from  $1 \times 10^8$  CFU/ml cell suspension combined with uninfected grape DNA in a 2:1 ratio. PCR consisted of 95°C for 3 min followed by 35 cycles of 95°C for 30 s and 60°C for 30 s. PCR was performed using a Bio-Rad CFX96 instrument. CFU/ml as determined by qPCR was normalized to total DNA concentration in ng/ $\mu$ l. Total DNA concentration of original samples was determined using Quant-iT dsDNA assay kit (Thermo Fisher).

**Data availability.** The data sets generated during this study are available on the Gene Expression Omnibus (GEO) database (<https://www.ncbi.nlm.nih.gov/geo/>) accession number (GSE184594).

## SUPPLEMENTAL MATERIAL

Supplemental material is available online only.

**SUPPLEMENTAL FILE 1**, PDF file, 0.5 MB.

## ACKNOWLEDGMENTS

We thank Brandon Ortega and Nathaniel Luna for technical support and Yaneth Barreto-Zavala for providing the images used for the grapevine symptoms rating scale. We also thank Leonardo De La Fuente and Marcus Merfa for helpful suggestions regarding imaging pili. Funding for this work was from United States Department of Agriculture (USDA) Agricultural Research Service appropriated project 2034-22000-012-00D. Mention of trade names or commercial products in this publication is solely for the purpose of providing specific information and does not constitute endorsement by USDA. USDA is an equal opportunity provider and employer.

## REFERENCES

1. Tumber K, Alston J, Fuller K. 2014. Pierce's disease costs California \$104 million per year. *Cal Ag* 68:20–29. <https://doi.org/10.3733/ca.v068n01p20>.
2. Schneider K, van der Werf W, Cendoya M, Mourits M, Navas-Cortés JA, Vicent A, Lansink AO. 2020. Impact of *Xylella fastidiosa* subspecies *pauca* in European olives. *Proc Natl Acad Sci U S A* 117:9250–9259. <https://doi.org/10.1073/pnas.1912206117>.
3. EFSA Panel on Plant Health. 2016. Treatment solutions to cure *Xylella fastidiosa* diseased plants. *EFSA J* 14:e04456.
4. White SM, Navas-Cortés JA, Bullock JM, Boscia D, Chapman DS. 2020. Estimating the epidemiology of emerging *Xylella fastidiosa* outbreaks in olives. *Plant Pathol* 69:1403–1413. <https://doi.org/10.1111/ppa.13238>.
5. Kottelenberg D, Hemerik L, Saponari M, van der Werf W. 2021. Shape and rate of movement of the invasion front of *Xylella fastidiosa* spp. *pauca* in Puglia. *Sci Rep* 11:1061. <https://doi.org/10.1038/s41598-020-79279-x>.
6. Hopkins DL, Purcell AH. 2002. *Xylella fastidiosa*: cause of Pierce's disease of grapevine and other emergent diseases. *Plant Dis* 86:1056–1066. <https://doi.org/10.1094/PDIS.2002.86.10.1056>.
7. Kyrkou I, Pusa T, Ellegaard-Jensen L, Sagot M-F, Hansen LH. 2018. Pierce's disease of grapevines: a review of control strategies and an outline of an epidemiological model. *Front Microbiol* 9:2141. <https://doi.org/10.3389/fmicb.2018.02141>.
8. Almeida RPP, Blua MJ, Lopes JRS, Purcell AH. 2005. Vector transmission of *Xylella fastidiosa*: applying fundamental knowledge to generate disease management strategies. *Ann Entomol Soc Am* 98:775–786. [https://doi.org/10.1603/0013-8746\(2005\)098\[0775:vtoxfa\]2.0.co;2](https://doi.org/10.1603/0013-8746(2005)098[0775:vtoxfa]2.0.co;2).
9. Ledbetter CA, Chen J, Livingston S, Groves RL. 2009. Winter curing of *Prunus dulcis* cv 'Butte,' *P. webbii* and their interspecific hybrid in response to *Xylella fastidiosa* infections. *Euphytica* 169:113–122. <https://doi.org/10.1007/s10681-009-9954-z>.
10. Lieth J, Meyer M, Yeo K-H, Kirkpatrick B. 2011. Modeling cold curing of Pierce's disease in *Vitis vinifera* 'Pinot Noir' and 'Cabernet Sauvignon' grapevines in California. *Phytopathology* 101:1492–1500. <https://doi.org/10.1094/PHYTO-08-10-0207>.
11. Yu T, Keto-Timonen R, Jiang X, Virtanen J-P, Korkeala H. 2019. Insights into the phylogeny and evolution of cold shock proteins: from enteropathogenic *Yersinia* and *Escherichia coli* to Eubacteria. *Int J Mol Sci* 20:4059. <https://doi.org/10.3390/ijms20164059>.
12. Michaux C, Holmqvist E, Vasicek E, Sharan M, Barquist L, Westermann AJ, Gunn JS, Vogel J. 2017. RNA target profiles direct the discovery of virulence functions for the cold-shock proteins CspC and CspE. *Proc Natl Acad Sci U S A* 114:6824–6829. <https://doi.org/10.1073/pnas.1620772114>.
13. Loepfe C, Raimann E, Stephan R, Tasara T. 2010. Reduced host cell invasiveness and oxidative stress tolerance in double and triple *csp* gene family deletion mutants of *Listeria monocytogenes*. *Foodborne Pathog Dis* 7:775–783. <https://doi.org/10.1089/fpd.2009.0458>.
14. Wu L, Ma L, Li X, Huang Z, Gao X. 2019. Contribution of the cold shock protein CspA to virulence in *Xanthomonas oryzae* pv. *oryzae*. *Mol Plant Pathol* 20:382–391. <https://doi.org/10.1111/mpp.12763>.
15. Yamanaka K, Inouye M. 1997. Growth-phase-dependent expression of *cspD*, encoding a member of the CspA family in *Escherichia coli*. *J Bacteriol* 179:5126–5130. <https://doi.org/10.1128/jb.179.16.5126-5130.1997>.
16. Burbank LP, Stenger DC. 2016. A temperature-independent cold-shock protein homolog acts as a virulence factor in *Xylella fastidiosa*. *Mol Plant Microbe Interact* 29:335–344. <https://doi.org/10.1094/MPMI-11-15-0260-R>.
17. Phadtare S, Tadigotla V, Shin W-H, Sengupta A, Severinov K. 2006. Analysis of *Escherichia coli* global gene expression profiles in response to over-expression and deletion of CspC and CspE. *J Bacteriol* 188:2521–2527. <https://doi.org/10.1128/JB.188.7.2521-2527.2006>.
18. Eshwar AK, Guldemann C, Oevermann A, Tasara T. 2017. Cold-shock domain family proteins (Csps) are involved in regulation of virulence, cellular aggregation, and flagella-based motility in *Listeria monocytogenes*. *Front Cell Infect Microbiol* 7:453. <https://doi.org/10.3389/fcimb.2017.00453>.
19. Caserta R, Takita MA, Targon ML, Rosselli-Murai LK, de Souza AP, Peroni L, Stach-Machado DR, Andrade A, Labate CA, Kitajima EW, Machado MA, de Souza AA. 2010. Expression of *Xylella fastidiosa* fimbrial and afimbrial proteins during biofilm formation. *Appl Environ Microbiol* 76:4250–4259. <https://doi.org/10.1128/AEM.02114-09>.

20. Li Y, Hao G, Galvani CD, Meng Y, Fuente LDLa, Hoch HC, Burr TJ. 2007. Type I and type IV pili of *Xylella fastidiosa* affect twitching motility, biofilm formation and cell–cell aggregation. *Microbiology* (Reading) 153:719–726. <https://doi.org/10.1099/mic.0.2006/002311-0>.
21. de Souza AA, Takita MA, Coletta-Filho HD, Caldana C, Yanai GM, Muto NH, de Oliveira RC, Nunes LR, Machado MA. 2004. Gene expression profile of the plant pathogen *Xylella fastidiosa* during biofilm formation *in vitro*. *FEMS Microbiol Lett* 237:341–353. <https://doi.org/10.1016/j.femsle.2004.06.055>.
22. Kandel PP, Chen H, Fuente LDL. 2018. A short protocol for gene knockout and complementation in *Xylella fastidiosa* shows that one of the type IV pilin paralogs (PD1926) is needed for twitching while another (PD1924) affects pilus number and location. *Appl Environ Microbiol* 84:e01167-18. <https://doi.org/10.1128/AEM.01167-18>.
23. Roper MC, Greve LC, Warren JG, Labavitch JM, Kirkpatrick BC. 2007. *Xylella fastidiosa* requires polygalacturonase for colonization and pathogenicity in *Vitis vinifera* grapevines. *Mol Plant Microbe Interact* 20:411–419. <https://doi.org/10.1094/MPMI-20-4-0411>.
24. De La Fuente L, Burr TJ, Hoch HC. 2008. Autoaggregation of *Xylella fastidiosa* cells is influenced by type I and type IV pili. *Appl Environ Microbiol* 74:5579–5582. <https://doi.org/10.1128/AEM.00995-08>.
25. Koczan JM, Lenneman BR, McGrath MJ, Sundin GW. 2011. Cell surface attachment structures contribute to biofilm formation and xylem colonization by *Erwinia amylovora*. *Appl Environ Microbiol* 77:7031–7039. <https://doi.org/10.1128/AEM.05138-11>.
26. Newman KL, Almeida RPP, Purcell AH, Lindow SE. 2003. Use of a green fluorescent strain for analysis of *Xylella fastidiosa* colonization of *Vitis vinifera*. *Appl Environ Microbiol* 69:7319–7327. <https://doi.org/10.1128/AEM.69.12.7319-7327.2003>.
27. Craig L, Forest KT, Maier B. 2019. Type IV pili: dynamics, biophysics and functional consequences. *Nat Rev Microbiol* 17:429–440. <https://doi.org/10.1038/s41579-019-0195-4>.
28. De La Fuente L, Montanes E, Meng Y, Li Y, Burr TJ, Hoch HC, Wu M. 2007. Assessing adhesion forces of type I and type IV pili of *Xylella fastidiosa* bacteria by use of a microfluidic flow chamber. *Appl Environ Microbiol* 73:2690–2696. <https://doi.org/10.1128/AEM.02649-06>.
29. Meng Y, Li Y, Galvani CD, Hao G, Turner JN, Burr TJ, Hoch HC. 2005. Upstream migration of *Xylella fastidiosa* via pilus-driven twitching motility. *J Bacteriol* 187:5560–5567. <https://doi.org/10.1128/JB.187.16.5560-5567.2005>.
30. Shi XY, Dumenyo CK, Hernandez-Martinez R, Azad H, Cooksey DA. 2009. Characterization of regulatory pathways in *Xylella fastidiosa*: genes and phenotypes controlled by *gacA*. *Appl Environ Microbiol* 75:2275–2283. <https://doi.org/10.1128/AEM.01964-08>.
31. Feng J-X, Song Z-Z, Duan C-J, Zhao S, Wu Y-Q, Wang C, Dow JM, Tang J-L. 2009. The *xrvA* gene of *Xanthomonas oryzae* pv. *oryzae*, encoding an HNS-like protein, regulates virulence in rice. *Microbiology* (Reading) 155:3033–3044. <https://doi.org/10.1099/mic.0.028910-0>.
32. Jaishankar J, Srivastava P. 2017. Molecular basis of stationary phase survival and applications. *Front Microbiol* 8:2000. <https://doi.org/10.3389/fmicb.2017.02000>.
33. Yamanaka K, Zheng W, Crooke E, Wang Y-H, Inouye M. 2001. CspD, a novel DNA replication inhibitor induced during the stationary phase in *Escherichia coli*. *Mol Microbiol* 39:1572–1584. <https://doi.org/10.1046/j.1365-2958.2001.02345.x>.
34. Wood TK, Knabel SJ, Kwan BW. 2013. Bacterial persister cell formation and dormancy. *Appl Environ Microbiol* 79:7116–7121. <https://doi.org/10.1128/AEM.02636-13>.
35. Prosser BL, Taylor D, Dix BA, Cleeland R. 1987. Method of evaluating effects of antibiotics on bacterial biofilm. *Antimicrob Agents Chemother* 31:1502–1506. <https://doi.org/10.1128/AAC.31.10.1502>.
36. González JF, Hahn MM, Gunn JS. 2018. Chronic biofilm-based infections: skewing of the immune response. *Pathog Dis* 76:fty023. <https://doi.org/10.1093/femspd/fty023>.
37. Kurniawan A, Yamamoto T. 2019. Accumulation of and inside biofilms of natural microbial consortia: implication on nutrients seasonal dynamic in aquatic ecosystems. *Int J Microbiol* 2019:e6473690. <https://doi.org/10.1155/2019/6473690>.
38. Kim Y, Wang X, Zhang X-S, Grigoriu S, Page R, Peti W, Wood TK. 2010. *Escherichia coli* toxin/antitoxin pair MqsR/MqsA regulate toxin CspD. *Environ Microbiol* 12:1105–1121. <https://doi.org/10.1111/j.1462-2920.2009.02147.x>.
39. Lee MW, Tan CC, Rogers EE, Stenger DC. 2014. Toxin-antitoxin systems *mqsR/ygiT* and *dinJ/reE* of *Xylella fastidiosa*. *Physiol Mol Plant Pathol* 87:59–68. <https://doi.org/10.1016/j.pmp.2014.07.001>.
40. Merfa MV, Niza B, Takita MA, De Souza AA. 2016. The MqsRA toxin-antitoxin system from *Xylella fastidiosa* plays a key role in bacterial fitness, pathogenicity, and persister cell formation. *Front Microbiol* 7:904. <https://doi.org/10.3389/fmicb.2016.00904>.
41. Chen J, Wu F, Zheng Z, Deng X, Burbank LP, Stenger DC. 2016. Draft genome sequence of *Xylella fastidiosa* subsp. *fastidiosa* strain Stag's Leap. *Genome Announc* 4. <https://doi.org/10.1128/genomeA.00240-16>.
42. Starr MP, Stolp H, Trüper HG, Balows A, Schlegel HG (ed). 1981. *The prokaryotes: a handbook on habitats, isolation and identification of bacteria*. Springer-Verlag, Berlin Heidelberg.
43. Kandel PP, Almeida RPP, Cobine PA, De La Fuente L. 2017. Natural competence rates are variable among *Xylella fastidiosa* strains and homologous recombination occurs *in vitro* between subspecies *fastidiosa* and *multiplex*. *Mol Plant Microbe Interact* 30:589–600. <https://doi.org/10.1094/MPMI-02-17-0053-R>.
44. Minsavage G, Thompson C, Hopkins D, Leite R, Stall R. 1994. Development of a polymerase chain reaction protocol for detection of *Xylella fastidiosa* in plant tissue. *Phytopathology* 84:456. <https://doi.org/10.1094/Phyto-84-456>.
45. Matsumoto A, Young GM, Igo MM. 2009. Chromosome-based genetic complementation system for *Xylella fastidiosa*. *Appl Environ Microbiol* 75:1679–1687. <https://doi.org/10.1128/AEM.00024-09>.
46. Voegel TM, Doddapaneni H, Cheng DW, Lin H, Stenger DC, Kirkpatrick BC, Roper MC. 2013. Identification of a response regulator involved in surface attachment, cell-cell aggregation, exopolysaccharide production and virulence in the plant pathogen *Xylella fastidiosa*: *Xylella* XhpT response regulator. *Mol Plant Pathol* 14:256–264. <https://doi.org/10.1111/mpp.12004>.
47. Merritt JH, Kadouri DE, O'Toole GA. 2005. Growing and analyzing static biofilms. *Curr Protoc Microbiol* Chapter 1:Unit 1B.1. <https://doi.org/10.1002/9780471729259.mc01b01s00>.
48. Wick RR, Judd LM, Holt KE. 2019. Performance of neural network basecalling tools for Oxford Nanopore sequencing. *Genome Biol* 20:129. <https://doi.org/10.1186/s13059-019-1727-y>.
49. Wick RR, Judd LM, Holt KE. 2018. Deepbin: demultiplexing barcoded Oxford Nanopore reads with deep convolutional neural networks. *PLoS Comput Biol* 14:e1006583. <https://doi.org/10.1371/journal.pcbi.1006583>.
50. Li H. 2018. Minimap2: pairwise alignment for nucleotide sequences. *Bioinformatics* 34:3094–3100. <https://doi.org/10.1093/bioinformatics/bty191>.
51. Patro R, Duggal G, Love MI, Irizarry RA, Kingsford C. 2017. Salmon: fast and bias-aware quantification of transcript expression using dual-phase inference. *Nat Methods* 14:417–419. <https://doi.org/10.1038/nmeth.4197>.
52. Sonese C, Love MI, Robinson MD. 2015. Differential analyses for RNA-seq: transcript-level estimates improve gene-level inferences. *F1000Res* 4:1521. <https://doi.org/10.12688/f1000research.7563.2>.
53. Love MI, Huber W, Anders S. 2014. Moderated estimation of fold change and dispersion for RNA-seq data with DESeq2. *Genome Biol* 15:550. <https://doi.org/10.1186/s13059-014-0550-8>.
54. Zaini PA, Fogaça AC, Lupo FGN, Nakaya HI, Vêncio RZN, da Silva AM. 2008. The iron stimulon of *Xylella fastidiosa* includes genes for type IV pilus and colicin V-like bacteriocins. *J Bacteriol* 190:2368–2378. <https://doi.org/10.1128/JB.01495-07>.
55. Ledbetter CA, Rogers EE. 2009. Differential susceptibility of prunus germplasm (subgenus *Amygdalus*) to a California isolate of *Xylella fastidiosa*. *Horts* 44:1928–1931. <https://doi.org/10.21273/HORTSCI.44.7.1928>.